Anionic Halomolybdate(III) Chemistry. Tetrahydrofuran Loss from $[MoX_3Y(THF)_2]^-$ (X, Y = Cl, Br, I), Preparation and Properties of $[Mo_3X_{12}]^{3-}$ (X = Br, I), and Crystal Structure of the Edge-Sharing Trioctahedral $[PPh_4]_3[Mo_3I_{12}]$

James C. Fettinger,[†] John C. Gordon,[†] Sundeep P. Mattamana,[†] Charles J. O'Connor,[‡] Rinaldo Poli,*[,†] and Ghadi Salem[†]

Department of Chemistry and Biochemistry, University of Maryland, College Park, Maryland 20742, and Department of Chemistry, University of New Orleans, New Orleans, Lousiana 70148

Received June 19, 1996[⊗]

By interaction of $MoX_3(THF)_3$ with [Cat]X in THF, the salts $[Cat][MoX_4(THF)_2]$ have been synthesized [X = I, Cat = PPh_4, NBu_4, NPr_4, $(Ph_3P)_2N$; X = Br, Cat = NBu_4, PPh_4 $(Ph_3P)_2N$]. Mixed-halide species $[MoX_3Y(THF)_2]^-$ (X, Y = Cl, Br, I) have also been generated in solution and investigated by ^{1}H-NMR. When the tetraiodo, tetrabromo, and mixed bromoiodo salts are dissolved in CH_2Cl_2, clean loss of all coordinated THF is observed by ^{1}H-NMR. On the other hand, $[MoCl_4(THF)_2]^-$ loses only 1.5 THF/Mo. The salts $[Cat]_3[Mo_3X_{12}]$ (X = Br, I) have been isolated from $[Cat][MoX_4(THF)_2]$ or by running the reaction between $MoX_3(THF)_3$ and [Cat]X directly in CH_2Cl_2. The crystal structure of $[PPh_4]_3[Mo_3I_{12}]$ exhibits a linear face-sharing trioctahedron for the trianion: triclinic, space group $P\bar{1}$; a = 11.385(2), b = 12.697(3), c = 16.849(2) Å; α = 76.65(2), β = 71.967(12), γ = 84.56(2)°; Z = 1; 431 parameters and 3957 data with $I > 2\sigma(I)$. The metal−metal distance is 3.258(2) Å. Structural and magnetic data are consistent with the presence of a metal−metal σ bond order of $^1/_2$ and with the remaining 7 electrons being located in 7 substantially nonbonding orbitals. The ground state of the molecule is predicted to be subject to a Jahn−Teller distortion, which is experimentally apparent from the nature of the thermal ellipsoid of the central Mo atom. The $[Mo_3X_{12}]^{3-}$ ions reacts with phosphines (PMe_3, dppe) to form products of lower nuclearity by rupture of the bridging Mo−X bonds.

Introduction

Coordination compounds of molybdenum(III) with ligands that do not possess strongly π-donating capabilities tend to adopt an octahedral coordination geometry. In the realm of molybdenum halide complexes, examples are (X = halide, L = neutral 2-electron donor) mononuclear octahedral MoX_3L_3,[1−11] $[MoX_4L_2]^-$,[10,12−14] and $[MoX_6]^{3-}$,[15,16] dinuclear edge-sharing bioctahedral $Mo_2X_6L_4$,[17−24] dinuclear face-sharing bioctahedral $Mo_2X_6L_3$,[22,25−27] $[Mo_2X_7L_2]^-$,[28,29] and $[Mo_2X_9]^{3-}$,[30−33] and the MoX_3 solids where one-third of the octahedral holes of the close-packed halide substructure are occupied by the metal atoms.[34,35] The occupied octahedral holes are arranged pairwise to give an infinite three-dimensional (for X = Cl) and monodimensional (for X = Br) $\{X_{3/2}Mo(\mu\text{-}X)_3MoX_{3/2}\}_\infty$ structure with localized Mo−Mo bonds. When one considers the hypothetical process of breaking apart the infinite MoX_3 structure by stepwise adding X^- ions, one should arrive directly, without breaking metal−metal bonds, at dinuclear $[Mo_2X_9]^{3-}$ units and then eventually to mononuclear $[MoX_6]^{3-}$. Indeed, the formation of $K_3Mo_2Cl_9$ and K_3MoCl_6 in a $KCl/TiCl_3/MoCl_3$ melt has been re-

[†] University of Maryland.
[‡] University of New Orleans.
[⊗] Abstract published in *Advance ACS Abstracts,* November 1, 1996.

(1) Allen, E. A.; Feenan, K.; Fowles, G. W. A. *J. Chem. Soc.* **1965**, 1636.
(2) Westland, A. D.; Muriithi, N. *Inorg. Chem.* **1972**, *11*, 2971.
(3) Anker, M. W.; Chatt, J.; Leigh, G. J.; Wedd, A. G. *J. Chem. Soc., Dalton Trans.* **1975**, 2639.
(4) Dilworth, J. R.; Richards, R. L. *Inorg. Synth.* **1980**, *20*, 119.
(5) Atwood, J. L.; Hunter, W. E.; Carmona-Guzman, E.; Wilkinson, G. *J. Chem. Soc., Dalton Trans.* **1980**, 467.
(6) Dilworth, J. R.; Zubieta, J. A. *J. Chem. Soc., Dalton Trans.* **1983**, 397.
(7) Roh, S.-Y.; Bruno, J. W. *Inorg. Chem.* **1986**, *25*, 3105.
(8) Cotton, F. A.; Poli, R. *Inorg. Chem.* **1987**, *26*, 1514.
(9) Owens, B. E.; Poli, R. *Polyhedron* **1989**, *8*, 545.
(10) Poli, R.; Gordon, J. C. *Inorg. Chem.* **1991**, *30*, 4550.
(11) Zeng, D.; Hampden-Smith, M. J. *Polyhedron* **1992**, *20*, 2585.
(12) Hills, A.; Leigh, G. J.; Hutchinson, J.; Zubieta, J. A. *J. Chem. Soc., Dalton Trans.* **1985**, 1069.
(13) Brencic, J. V.; Ceh, B.; Leban, I. *Z. anorg. allg. Chem.* **1986**, *538*, 212.
(14) Brencic, J. V.; Modec, B. *Z. Anorg. Allg. Chem.* **1994**, *620*, 950.
(15) Rosenheim, R.; Tsu, H. L. *Ber. Dtsch. Chem. Ges.* **1923**, *56*, 2228.
(16) Kusak'baev, A.; Parpiev, N. A.; Ismailov, M.; Ahmedova, B. C.; Tohtasev, G.; Terishanova, I. G.; Jusupova, N. K. *Koord. Khim.* **1983**, *9*, 808.
(17) Cotton, F. A.; Fanwick, P. E.; Fitch, J. W., III. *Inorg. Chem.* **1978**, *17*, 3254.
(18) Cotton, F. A.; Diebold, M. P.; O'Connor, C. J.; Powell, G. L. *J. Am. Chem. Soc.* **1985**, *107*, 7438.
(19) Chakravarty, A. R.; Cotton, F. A.; Diebold, M. P.; Lewis, D. B.; Roth, W. J. *J. Am. Chem. Soc.* **1986**, *108*, 971.
(20) Agaskar, P. A.; Cotton, F. A.; Dunbar, K. R.; Falvello, L. R.; O'Connor, C. J. *Inorg. Chem.* **1987**, *26*, 4051.
(21) Mui, H. D.; Poli, R. *Inorg. Chem.* **1989**, *28*, 3609.
(22) Poli, R.; Mui, H. D. *Inorg. Chem.* **1991**, *30*, 65.
(23) Cotton, F. A.; Daniels, L. M.; Dunbar, K. R.; Falvello, L. R.; O'Connor, C. J.; Price, A. C. *Inorg. Chem.* **1991**, *30*, 2509.
(24) Poli, R.; Gordon, J. C. *J. Am. Chem. Soc.* **1992**, *114*, 6723.
(25) Moynihan, K. J.; Gao, X.; Boorman, P. M.; Fait, J. F.; Freeman, G. K. W.; Thornton, P.; Ironmonger, D. J. *Inorg. Chem.* **1990**, *29*, 1648.
(26) Cotton, F. A.; Luck, R. L.; Son, K.-A. *Inorg. Chim. Acta* **1990**, *173*, 131.
(27) Ahmed, K. J.; Gordon, J. C.; Mui, H. D.; Poli, R. *Polyhedron* **1991**, *10*, 1667.
(28) Cotton, F. A.; Poli, R. *Inorg. Chem.* **1987**, *26*, 3310.
(29) Cotton, F. A.; Luck, R. L. *Inorg. Chem.* **1989**, *28*, 182.
(30) Saillant, R. B.; Streib, W. E.; Foltong, K.; Wentworth, R. A. D. *Inorg. Chem.* **1971**, *10*, 1453.
(31) Saillant, R.; Wentworth, R. A. *Inorg. Chem.* **1969**, *8*, 1226.
(32) Dubicki, L.; Krausz, E.; Stranger, R.; Smith, P. W.; Tanabe, Y. *Inorg. Chem.* **1987**, *26*, 2247.
(33) Stranger, R.; Smith, P. W.; Grey, I. E. *Inorg. Chem.* **1989**, *28*, 1271.
(34) Schäfer, H.; von Schnering, H.-G.; Tillack, J.; Kuhnen, F.; Wöhrle, H.; Baumann, H. Z. *Z. Anorg. Allg. Chem.* **1967**, *353*, 281.
(35) Babel, D. *J. Solid State Chem.* **1972**, *4*, 410.

S0020-1669(96)00730-6 CCC: $12.00

ported.[36] About 20 years ago a related ion, $[Mo_3Cl_{12}]^{3-}$, has also been described.[37] This was obtained by combining $[Mo_2Cl_9]^{2-}$ and $[MoCl_3(CO)_4]^-$ in a 1:1 ratio and was proposed to adopt a face-sharing trioctahedral structure on the basis of optical, magnetic, and conductivity studies. This structure is not related to a fragment of the $MoCl_3$ solid and an interesting question concerns the extent of metal−metal bonding along the supposed linear Mo_3 unit.

We have recently become aware that the convenient starting materials $MoX_3(THF)_3$ have a marked tendency to lose THF in noncoordinating solvents to afford edge-sharing bioctahedral $Mo_2X_6(THF)_4$ and ultimately face-sharing bioctahedral $Mo_2X_6(THF)_3$ (X = Cl, Br).[38] We have also found that $MoCl_3(THF)_3$ readily reacts with Cl^- in THF to provide the mononuclear complex *trans*-$[MoCl_4(THF)_2]^-$.[10] We therefore recognized the possibility of utilizing this strategy as a new entry into halomolybdate(III) ions. Here we report our studies on the interaction between $MoX_3(THF)_3$ and Y^- ions (X, Y = Cl, Br, I) and the THF loss from the resulting complexes which led to the formation of $[Mo_3X_{12}]^{3-}$ (X = Br, I), and we present the trioctahedral structure of the iodo complex. The products obtained upon reaction of these trinuclear materials with unidentate and bidentate phosphine ligands are also described. A preliminary account of part of this work has appeared.[39]

Experimental Section

All operations were carried out under a dinitrogen atmosphere by using standard glovebox and Schlenk-line techniques. Solvents were purified by conventional methods and distilled under dinitrogen prior to use. ^{1}H-NMR measurements were carried out in thin-walled 5 mm NMR tubes with a Bruker WP200 spectrometer. EPR spectra were carried out in 4 mm quartz tubes with a Bruker ER200 spectrometer equipped with an X-band microwave generator and the spectra were calibrated with DPPH. Magnetic measurements at room temperature were carried out by a modified Gouy method with the commercially available (Johnson Matthey) magnetic balance, while the variable-temperature magnetic susceptibility data on compounds $[PPh_3]_3[Mo_3X_{12}]$ (X = Br, I) were recorded on 24.38 and 29.22 mg polycrystalline samples, respectively, over the 1.7-300 K temperature region using a Quantum Design MPMS-5S SQUID susceptometer at a magnetic field of 1000 G. Measurement and calibration techniques have been reported elsewhere.[40] Cyclic voltammograms were recorded with an EG&G 362 potentiostat connected to a Macintosh computer through MacLab hardware/software; the electrochemical cell was a locally modified Schlenk tube with a Pt counterelectrode sealed through uranium glass/Pyrex glass seals. The cell was fitted with a Ag/AgCl reference electrode and a Pt working electrode. All measurements were carried out with *n*-Bu_4NPF_6 (ca. 0.1 M) as the supporting electrolyte, and all potentials are reported vs the Cp_2Fe/Cp_2Fe^+ couple which was introduced into the cell at the end of each measurement. IR spectra in the 4000−400 cm^{-1} region were recorded in Nujol mulls with KBr optics on a Perkin-Elmer 1800 spectrophotometer. Low-energy IR spectra (400−100 cm^{-1} region) were recorded in Nujol mulls with CsI optics on a Perkin-Elmer 1800 spectrophotometer. Micro-Raman spectra were recorded at room temperature using a Raman triple spectrometer (Instruments SA) with a coherent Innova 301 Kr^+ laser. Elemental analyses were from M-H-W Laboratories, Phoenix, AZ.

Compounds $MoCl_3(THF)_3$,[6] $MoBr_3(THF)_3$,[9] and $MoI_3(THF)_3$[8] were prepared according to the literature procedures or, for the trichloride system, to a modification[10] of the literature procedure.

^{1}H-NMR Monitoring of $MoX_3(THF)_3 + Y^-$ Reactions (X, Y = Cl, Br, I). Each reaction was set up in an NMR tube a similar fashion. Ca. 20 mg of $MoX_3(THF)_3$ and the stoichiometric quantity of a salt of Y^- [the salts PPh_4Y (Y = Cl, I) and NBu_4Y (Y = Cl, Br, I) were used] were placed in a thin-walled 5 mm NMR tube. The tube was cooled to −78 °C, and ca. 1 mL of $CDCl_3$ or CD_2Cl_2 was added. The tube was maintained at the dry-ice temperature until introduction into the NMR probe. The transformation of *mer*-$MoX_3(THF)_3$ to *mer*,*trans*-$[MoX_3Y(THF)_2]^-$ was complete within 10 min in each case. The ^{1}H-NMR resonances of the products are collected in Table 1. However, the reactions progress further to release additional THF; see Results.

Table 1. Room-Temperature ^{1}H-NMR Resonances for the Coordinated THF Ligands in $[MoX_3Y(THF)_2]^-$ Complexes[a]

		^{1}H-NMR [δ/ppm ($w_{1/2}$/Hz)]	
X	Y	α-H	β-H
Cl	Cl	72 (1100)	8.3 (185)
Cl	Br	75 (1800)	8.5 (225)
Cl	I	79 (870)	8.5 (265)
Br	Cl	82 (1050)	9.0 (190)
Br	Br	83 (1100)	9.0 (220)
Br	I	84 (1200)	9.4 (360)
I	Cl	96 (890)	11.3 (100)
I	Br	96 (1400)	11.3 (230)
I	I[b]	100 (840)	12.5 (150)

[a] Solvent = $CDCl_3$ unless otherwise specified. [b] In CD_2Cl_2.

Preparation of $[Ph_4P][MoI_4(THF)_2]$. $MoI_3(THF)_3$ (507 mg, 0.73 mmol) and PPh_4I (341 mg, 0.73 mmol) were placed in a Schlenk tube to which THF (20 mL) was subsequently added. The slurry was magnetically stirred overnight at room temperature resulting in the formation of a green precipitate. The precipitate was filtered, washed with THF, and dried under vacuum. Yield: 582 mg, 73%. Anal. Calcd for $C_{32}H_{36}I_4MoPO_2$: C, 35.32; H, 3.34. Found: C, 35.7; H, 3.7. The ^{1}H-NMR of this material is reported in Table 1.

Preparation of $[Bu_4N][MoI_4(THF)_2]$. By a procedure analogous to that described above for the preparation of the PPh_4 salt, $MoI_3(THF)_3$ (653 mg, 0.94 mmol) and NBu_4I (348 mg, 0.94 mmol) in 30 mL of THF gave 636 mg of green product (68%). Anal. Calcd for $C_{24}H_{52}I_4MoNO_2$: C, 29.12; H, 5.30. Found: C, 29.4; H, 5.6.

Preparation of $[Pr_4N][MoI_4(THF)_2]$. By a procedure analogous to that described above for the preparation of the PPh_4 salt, $MoI_3(THF)_3$ (511 mg, 0.73 mmol) and NPr_4I (230 mg, 0.73 mmol) in 25 mL of THF gave 334 mg of green product (49%). Anal. Calcd for $C_{20}H_{44}I_4MoNO_2$: C, 25.71; H, 4.75. Found: C, 25.8; H, 4.7.

Preparation of $[PPN][MoI_4(THF)_2]$. By a procedure analogous to that described above for the preparation of the PPh_4 salt, $MoI_3(THF)_3$ (306 mg, 0.44 mmol) and PPNI (294 mg, 0.44 mmol) in 15 mL of THF gave 471 mg of green product (82%). Anal. Calcd for $C_{44}H_{48}I_4MoNO_2P_2$: C, 41.02; H, 3.76. Found: C, 40.8; H, 3.6.

^{1}H-NMR Monitoring of the THF Loss from $[MoI_4(THF)_2]^-$ in $CDCl_3$. In separate experiments, a small amount (ca. 20 mg) of each $[MoI_4(THF)_2]^-$ salt (with the PPh_4^+, NBu_4^+ and NPr_4^+ cations, respectively) was introduced in a 4-mm thin-walled NMR tube. Ca. 1 mL of $CDCl_3$ was introduced while maintaining the tube at the dry-ice temperature, and the tube was warmed up to room temperature only immediately prior to the introduction into the NMR probe. The resonances attributed to the coordinated THF (see Table 1) were evident at the initial times in each case, but they rapidly decreased and were replaced by new resonances of equal intensity in the region expected for free THF (α-H, δ 3.7−3.9; β-H, δ 1.8−2.0; the slight variability of chemical shift for these resonances is probably due to changes in the bulk magnetic susceptibility of the solution). Correspondingly, a shift of the resonances due to the cation protons to lower fields and a broadening of the same resonances was observed. PPh_4 salt: from 7.7 ($w_{1/2}$ = 80 Hz) to 9.0 ($w_{1/2}$ = 600 Hz). NBu_4 salt: $N(CH_2CH_2CH_2CH_3)_4$, from ca. 1.5 to 3.1 ($w_{1/2}$ = 35 Hz); $N(CH_2CH_2CH_2CH_3)_4$, from ca. 1.2 to 1.7 ($w_{1/2}$ ca. 30 Hz); $N(CH_2CH_2CH_2CH_3)_4$, from ca. 1.2 to 1.5 ($w_{1/2}$ ca. 20 Hz); $N(CH_2CH_2CH_2CH_3)_4$, from ca. 1.0 to 1.0 ($w_{1/2}$ = 18 Hz). NPr_4 salt: $N(CH_2CH_2CH_3)_4$; from ca. 1.6 to 3.2 ($w_{1/2}$ = 70 Hz); $N(CH_2CH_2CH_3)_4$; from ca. 1.2 to ca. 2.2 (overlap with THF β-H resonance); $N(CH_2CH_2CH_3)_4$; from ca. 1.0 to 1.2 ($w_{1/2}$ = 30 Hz).

(36) *Gmelin Handbook of Inorganic Chemistry*; Springer-Verlag: Berlin, 1990; Vol. Mo Supp. Vol 5B, p 296.
(37) Delphin, W. H.; Wentworth, R. A. D.; Matson, M. S. *Inorg. Chem.* **1974**, *13*, 2552.
(38) Poli, R.; Mui, H. D. *J. Am. Chem. Soc.* **1990**, *112*, 2446.
(39) Fettinger, J. C.; Mattamana, S. P.; O'Connor, C. J.; Poli, R.; Salem, G. *J. Chem. Soc., Chem. Commun.* **1995**, 1265.
(40) O'Connor, C. J. *Prog. Inorg. Chem.* **1982**, *29*, 203.

The transformation was most rapid for the NPr_4 salt (<20 min), intermediate for the NBu_4 salt (ca. 30 min), and slower for the PPh_4 salt (ca. 1 h).

Preparation of $[Ph_4P]_3[Mo_3I_{12}]$. $MoI_3(THF)_3$ (432 mg, 0.62 mmol) was introduced in a Schlenk tube and slurried in CH_2Cl_2 (10 mL). To this suspension was added dropwise a solution containing PPh_4I (272 mg, 0.58 mmol) in CH_2Cl_2 (10 mL) while stirring at room temperature. A dark brown solution resulted at the end of the addition. After filtration, the solution was concentrated to ca. 10 mL and toluene (15 mL) was added. The brown precipitated that was formed was filtered off, washed with toluene (10 mL), and dried under vacuum. Yield: 454 mg (78%). Anal. Calcd for $C_{24}H_{20}I_4MoP$: C, 30.56; H, 2.14. Found: C, 30.7; H, 2.3. μ_{eff} (298 K) = 1.83 μ_B/Mo atom. The compound is EPR silent at room temperature and at 77 K. Low-energy IR (Nujol mull, cm^{-1}): 251 s, 226 m, 190 w, 179 m. Raman (cm^{-1}): 169 s, 113 s.

A single crystal of this compound was obtained by dissolving a mixture of $[PPh_4][MoI_4(THF)_2]$ (230 mg, 0.21 mmol) and PPh_4I (105 mg, 0.22 mmol) in 5 mL of CH_2Cl_2 and then carefully layering the resulting solution with diethyl ether (5 mL). Diffusion was initially allowed to take place at room temperature. After 1 day, single crystals started to form and the diffusion was continued at −20 °C to complete the crystallization.

Preparation of $[Bu_4N]_3[Mo_3I_{12}]$. $MoI_3(THF)_3$ (984 mg, 1.42 mmol) and NBu_4I (525 mmol, 1.42 mmol) were placed in a Schlenk tube. CH_2Cl_2 (15 mL) was added, and the mixture was stirred at room temperature for ca. 1 h, resulting in the formation of a brown solution. Cooling to 0 °C resulting in the formation of a microcrystalline precipitate, which was filtered and dried under vacuum (322 mg). Anal. Calcd for $C_{16}H_{36}I_4MoN$: C, 22.72; H, 4.29. Found: C, 22.8; H, 4.5. Low-energy IR (Nujol mull, cm^{-1}): 249 s, 215 m, 198 w, 174 m. Raman (cm^{-1}): 170 s, 110 s. From the mother solution, a further crop of solid (594 mg) was obtained upon addition of Et_2O (20 mL), bringing the total yield to 76%.

Preparation of $[Pr_4N]_3[Mo_3I_{12}]$. By a procedure identical to that described above for the analogous Bu_4N^+ salt, $MoI_3(THF)_3$ (541 mg, 0.78 mmol) and Pr_4NI (245 mg, 0.78 mmol) in 20 mL of CH_2Cl_2 gave 450 mg of product (73% yield). Anal. Calcd for $C_{12}H_{28}I_4MoN$: C, 18.25; H, 3.57. Found: C, 18.6; H, 3.6. μ_{eff} (298 K) = 1.94 μ_B/Mo atom. Low-energy IR (Nujol mull, cm^{-1}): 210 s, 189 m.

Preparation of $[PPN]_3[Mo_3I_{12}]$. By a procedure identical to that described above for the analogous Bu_4N^+ salt, $MoI_3(THF)_3$ (244 mg, 0.35 mmol) and PPNI (240 mg, 0.36 mmol) in 10 mL of CH_2Cl_2 gave a brown solution. The compound did not crystallize from this solution at room temperature or upon cooling and addition of pentane caused the formation of oily material. Therefore, the solution was evaporated to dryness and the residue was repeatedly washed with pentane and finally dried under vacuum. A 357 mg amount of product (81% yield) was obtained. The product is not analytically pure; however its elemental analysis corresponds closely to that calculated for $[PPN]_3[Mo_3I_{12}]\cdot 4.5$ THF. Anal. Calcd for $C_{42}H_{42}I_4MoNO_{1.5}P_2$: C, 40.35; H, 3.38. Found: C, 40.0; H, 3.6. The presence of free THF in the isolated material was confirmed by ^{1}H-NMR.

Preparation of $[Bu_4N][MoBr_4(THF)_2]$. $MoBr_3(THF)_3$ (371 mg, 0.67 mmol) and Bu_4NBr (215 mg, 0.67 mmol) were placed in a Schlenk tube equipped with a magnetic stirrer bar. THF (10 mL) was added, and the resulting suspension was stirred at room temperature. After ca. 30 min, the solid completely dissolved to afford a red solution. Stirring was allowed to continue overnight, after which time a pink precipitate had formed. This solid was collected by filtration, washed with *n*-heptane (10 mL), and dried under vacuum. Yield: 374 mg, 70%. Anal. Calcd for $C_{24}H_{52}Br_4MoNO_2$: C, 36.26; H, 6.31. Found: C, 35.9; H, 6.5. This solid is only sparingly soluble in THF and soluble in $CHCl_3$ and CH_2Cl_2. Its NMR in $CDCl_3$ (anion) is identical with that observed during the NMR monitoring of the $MoBr_3(THF)_3/Br^-$ reaction (vide supra) and is reported in Table 1.

Preparation of $[PPN][MoBr_4(THF)_2]$. By a procedure analogous to that reported above for the corresponding Bu_4N^+ salt, $MoBr_3(THF)_3$ (597 mg, 1.08 mmol) and PPNBr (669 mg, 1.08 mmol) in 15 mL of THF afforded 610 mg (51.4%) of pink product. Anal. Calcd for $C_{44}H_{48}Br_4MoNO_2P_2$: C, 48.11; H, 4.22. Found: C, 48.1; H, 4.8.

Preparation of $[PPh_4][MoBr_4(THF)_2]$. By a procedure analogous to that reported above for the corresponding Bu_4N^+ salt, $MoBr_3(THF)_3$ (742 mg, 1.35 mmol) and PPh_4 (575 mg, 1.35 mmol) in 30 mL of THF afforded 998 mg (81.3%) of pink product. Anal. Calcd for $C_{32}H_{36}Br_4MoO_2P$: C, 42.74; H, 4.03. Found: C, 42.90; H, 4.31.

^{1}H-NMR Monitoring of the THF loss from $[MoBr_4(THF)_2]^-$ in CD_2Cl_2. $[PPN][MoBr_4(THF)_2]$ (15 mg, 0.014 mmol) was placed in an NMR tube, and 1 mL of CD_2Cl_2 was introduced while maintaining the tube at dry-ice temperature. The sample was kept cold until the introduction into the NMR probe for the reaction monitoring at room temperature. Monitoring by ^{1}H-NMR indicated the same behavior described above for the analogous experiment on the corresponding tetraiodo salts [clean evolution of 2 mol of free THF per Mo atom (δ 3.71 for α-H; δ 1.83 for β-H)]. The PPN resonances were observed in the δ 7.8−7.2 region and did not significantly shift during the reaction, which was complete in about 7 h.

Preparation of $[PPN]_3[Mo_3Br_{12}]$. $MoBr_3(THF)_3$ (357 mg, 0.65 mmol) and PPNBr (400 mg, 0.65 mmol) in CH_2Cl_2 gave a red-brown solution. The solid was precipitated from solution by the addition of Et_2O, filtered off, washed with Et_2O, and dried under vacuum. Yield: 331 mg, 54%. Anal. Calcd for $C_{36}H_{30}Br_4MoNP_2$: C, 45.32; H, 3.17. Found: 45.6; H, 3.8. Low-energy IR (Nujol mull, cm^{-1}): 255 cm^{-1}.

Preparation of $[Bu_4N]_3[Mo_3Br_{12}]$. $MoBr_3(THF)_3$ (595 mg, 1.07 mmol) and Bu_4Br (350 mg, 1.08 mmol) were placed in a Schlenck tube, and to this was added 15 mL of CH_2Cl_2. The red-brown solution which formed was stirred overnight. The solution was then concentrated to ca. 5 mL and the solid precipitated by addition of 20 mL of ether, filtered off, washed with ether, and dried under vacuum. Yield: 642 mg, 90.4%. Anal. Calcd for $C_{16}H_{36}Br_4MoN$: C, 29.20; H, 5.51. Found: 30.43; H, 6.04. Low-energy IR (Nujol mull, cm^{-1}): 252, 215. μ_{eff} = 1.14 μ_B/Mo atom. The compound is air sensitive, and exposure to air modifies the IR spectrum to give rise to the following new bands: 995 s, 290 s, 257 s.

Preparation of $[PPh_4]_3[Mo_3Br_{12}]$. $MoBr_3(THF)_3$ (803 mg, 1.45 mmol) and PPh_4Br (615 mg, 1.46 mmol) were placed in a Schlenck tube to which 25 mL of CH_2Cl_2 was added at room temperature. After ca. 1 h of stirring you could see formation of a pink precipitate. The mixture was stirred for ca. 4 h, and the precipitate was filtered out, washed with CH_2Cl_2, and dried under vacuum. Yield: 865 mg, 78.9%. Anal. Calcd for $C_{24}H_{20}Br_4MoP$: C, 38.10; H, 2.60. Found: 38.07; H, 3.02. μ_{eff} = 1.50 μ_B/Mo atom.

^{1}H-NMR Monitoring of the THF Loss from $[MoCl_4(THF)_2]^-$ in CD_2Cl_2. $[PPN]^+[MoCl_4(THF)_2]^-$ (15 mg, 0.016 mmol) was introduced in a 4-mm thin-walled NMR tube. Ca. 1 mL of CD_2Cl_2 was introduced while maintaining the tube at the dry-ice temperature, and the tube was warmed to room temperature prior to the introduction into the NMR probe. Free THF (δ 3.69, α-H; δ 1.81, β-H) formed slowly and leveled off to 1.4 equiv of THF per Mo atom overnight. At the same time, the THF resonances of the mononuclear starting material (Table 1) were replaced by new resonances at δ 6.7 (α-H, $w_{1/2}$ = 38 Hz) and 2.2 (β-H, $w_{1/2}$ = 14 Hz), which correspond to ca. 0.5 THF molecules per Mo atom. At large amplifications, a small resonance at δ 17 ($w_{1/2}$ = 165 Hz) was also observed.

Reactions between $[Mo_3X_{12}]^{3-}$ Salts and Phosphines (PMe_3, dppe). (1) with PMe_3. (a) $[PPh_4]_3[Mo_3I_{12}]$. The tetraphenylphosphonium salt (259 mg, 0.092 mmol) was dissolved in 15 mL of CH_2Cl_2, and to the resulting solution was added PMe_3 (55 μL, ca. 0.55 mmol). The mixture was stirred at room temperature for 3 h, after which time a ^{1}H-NMR spectrum on an aliquot of the solution (CD_2Cl_2) showed the following resonances (relative intensities in parentheses): δ −2.18 and −2.84 (17% and 24%; $w_{1/2}$ = 7 and 11 Hz; *syn* and *gauche* $[Mo_2I_7(PMe_3)_2]^-$), −20.8 and −30.9 (16% and 32%; $w_{1/2}$ = 103 and 118 Hz; *mer*-$MoI_3(PMe_3)_3$); −41 (11%; $w_{1/2}$ = 154 Hz; *trans*-$[MoI_4(PMe_3)_2]^-$). Two additional resonances due to the reaction product of PMe_3 and CH_2Cl_2 are also observed at δ 2.2 ($[Me_3PCH_2Cl]^+$) and 1.8 ($[Me_3PCH_2Cl]^+$).

An analogous result was obtained when $[PPN]_3[Mo_3I_{12}]$ or $[NBu_4]_3[Mo_3I_{12}]$ were used instead of the PPh_4 salt under otherwise identical conditions. The same result was also obtained when the PPh_4 salt was obtained in situ from $[PPh_4][MoI_4(THF)_2]$ in CH_2Cl_2 as described above. When, on the other hand, the $[PPh_4][MoI_4(THF)_2]$ salt was dissolved in CH_2Cl_2 and the resulting solution immediately cooled to −80 °C and reacted with PMe_3 (2 equiv) (that is, before extensive transformation

to the $[Mo_3I_{12}]^{3-}$ salt could occur; *vide supra*), then the $[MoI_4(PMe_3)_2]^-$ species (^{1}H-NMR resonance at δ −41) was the dominant product (>85% of the integrated ^{1}H-NMR resonances).

(b) [PPN]$_3$[Mo$_3$Br$_{12}$]. The compound was prepared in situ as described above from $MoBr_3(THF)_3$ (180 mg, 0.33 mmol) and PPNBr (202 mg, 0.33 mmol) in 20 mL of CH_2Cl_2. To the resulting solution was added PMe_3 (66 μL, ca. 0.66 mmol), following by stirring at room temperature for 3 h. A small amount of a pink precipitate formed immediately, and the color of the solution changed from red-brown to purple. An aliquot of the solution was investigated by ^{1}H-NMR (relative intensities in parentheses): δ −1.20 and −1.70 (8% and 35%; $w_{1/2}$ = 40 and 32 Hz; *syn* and *gauche* $[Mo_2Br_7(PMe_3)_2]^-$), −19.5 and −33.0 (5% and 8%; $w_{1/2}$ = 184 and 211 Hz; *mer*-$MoBr_3(PMe_3)_3$); −40.8 (44%; $w_{1/2}$ = 250 Hz; *trans*-$[MoBr_4(PMe_3)_2]^-$). Two additional resonances due to the reaction product of PMe_3 and CH_2Cl_2 are also observed at δ 2.2 ($[Me_3PCH_2Cl]^+$) and 1.8 ($[Me_3PCH_2Cl]+$).

(2) with dppe. (a) [PPh$_4$]$_3$[Mo$_3$I$_{12}$]. $[PPh_4]_3[Mo_3I_{12}]$ (70 mg, 0.025 mmol) was dissolved in 10 mL of CH_2Cl_2. To this solution was added dppe (35 mg, 0.087 mmol) at room temperature, and the mixture was stirred for ca. 3 h. An aliquot of this solution was used for NMR studies in CD_2Cl_2. The ^{1}H-NMR spectrum showed the following resonances: δ 21.55 (br s, $w_{1/2}$ = 160 Hz, *o*-Ph of dppe), 10.3 (br s, $w_{1/2}$ = 32 Hz, *m*-Ph of dppe), 10.1 (br s, $w_{1/2}$ = 32 Hz, *p*-Ph of dppe), 7.3 (m, PPh_4), −21.6 (br s, $w_{1/2}$ = 280 Hz, CH_2 of dppe) which is attributed to *cis*-$[PPh_4][MoI_4(dppe)]$. A resonance at δ 35.73 due to $Mo_2I_6(dppe)_2$ was also observed in the ^{31}P NMR.

(b) [Bu$_4$N][Mo$_3$Br$_{12}$]. By a procedure identical to that described above for the analogous salt $[PPh_4]_3[Mo_3I_{12}]$, $[Bu_4N][Mo_3Br_{12}]$ (53 mg, 0.027 mmol) and dppe (35 mg, 0.087 mmol) were combined in 10 mL of CH_2Cl_2. ^{1}H-NMR (δ, CD_2Cl_2, room temperature): δ 18.10 (br s, $w_{1/2}$ = 320 Hz, *o*-Ph of dppe), 10.4 (br s, $w_{1/2}$ = 48 Hz, *m*-Ph of dppe), 9.71 (br s, $w_{1/2}$ = 32 Hz, *p*-Ph of dppe), 1.0, 1.8, 1.9, 3.1 (br, Bu_4N), −25.9 (br s, $w_{1/2}$ = 400 Hz, CH_2 of dppe) which is attributed to *cis*-$[Bu_4N][MoBr_4(dppe)]$. A resonance at δ 39.6 due to $Mo_2Br_6(dppe)_2$ was also observed in the ^{31}P-NMR.

(c) [PPh$_4$]$_3$[Mo$_3$Br$_{12}$]. $[PPh_4]_3[Mo_3Br_{12}]$ (65mg, 0.029 mmol) was treated with 5 mL of CH_2Cl_2. To this mixture was added dppe (40 mg, 0.10 mmol) dissolved in 5 mL of CH_2Cl_2. This mixture was let to stir overnight, resulting in the complete dissolution of $[PPh_4]_3[Mo_3Br_{12}]$ to afford a red solution. An aliquot was used for NMR studies in CD_2Cl_2. The ^{1}H-NMR spectrum showed the following resonances: δ 18.70 (br s, $w_{1/2}$ = 360 Hz, *o*-Ph of dppe), 10.68 (br s, $w_{1/2}$ = 99 Hz, *m*-Ph of dppe), 9.8 (br s, $w_{1/2}$ = 96 Hz, *p*-Ph of dppe), 7.5 (m, PPh4), −25.3 (br s, $w_{1/2}$ = 416 Hz, CH_2 of dppe) which is attributed to *cis*-$[PPh_4][MoBr_4(dppe)]$. A resonance at δ 39.9 due to $Mo_2Br_6(dppe)_2$ was also observed in the ^{31}P-NMR.

Preparation of [PPh$_4$][MoI$_4$(PMe$_3$)$_2$]. $[PPh_4][MoI_4(THF)_2]$ (185 mg, 0.17 mmol) was placed in a Schlenk tube and dissolved in CH_2Cl_2 (25 mL) at −80 °C. To the resulting solution was added PMe_3 (340 μL, 0.34 mmol), and the reaction mixture was allowed to slowly warm to room temperature, during which time the color changed from green to red-brown, and stirred further at room temperature for 2 h. The ^{1}H-NMR of an aliquot of the solution showed, in addition to the major resonance of the product at δ −41.2 ($w_{1/2}$ = 200 Hz), also minor resonances at −20.9 and −31.2 in a 1:2 ratio, assigned to $MoI_3(PMe_3)_3$,[22] and at δ −2.18 and −2.84, assigned to the *anti*- and *gauche*-$[Mo_2I_7(PMe_3)_2]^-$ ions, respectively.[28] After filtration, the solution was evaporated to dryness and the residue was extracted with 15 mL of chloroform. The yellow precipitate which remained undissolved was washed with chloroform and dried under vacuum. Yield: 87 mg (45.5%). Anal. Calcd for $C_{32}H_{42}MoI_4P_3O_{0.5}$ ($[PPh_4][MoI_4(PMe_3)_2]\cdot$ 0.5THF: C, 34.0; H, 3.7. Found: C, 34.3; H, 3.6. The presence of THF was confirmed by ^{1}H-NMR, which also showed the absence of the other Mo phosphine complexes previously present in the reaction mixture.

Preparation of [PPN][MoBr$_4$(dppe)]. $MoBr_3(dppe)(THF)$ was prepared in situ by reacting $MoBr_3(THF)_3$ (380 mg, 0.69 mmol) and dppe (275 mg, 0.69 mmol) in 30 mL of THF. This solution was then evaporated to dryness, and to this residue was added PPNBr (400 mg, 0.70 mmol) dissolved in 25 mL of CH_2Cl_2. The residue dissolved completely forming a red-brown solution. The reaction was complete in 2 h, as verified by NMR monitoring. The solution was then concentrated to ca. 5 mL and the product precipitated by addition of 20 mL of ether. The orange solid was washed with ether and dried under vacuum. Yield: 675 mg, 72.5%. Anal. Calcd for $C_{62}H_{54}Br_4MoNP_4$: C, 55.12; H, 4.02. Found: C, 55.85; H, 4.31. ^{1}H-NMR (δ, CD_2Cl_2, room temperature): δ 19.06 (br s, $w_{1/2}$ = 368 Hz, *o*-Ph of dppe), 10.89 (br s, $w_{1/2}$ = 45 Hz, *m*-Ph of dppe), 9.8 (br s, $w_{1/2}$ = 28 Hz, *p*-Ph of dppe), 7.54 (m, PPh_4), −25.48 (br s, $w_{1/2}$ = 530 Hz, CH_2 of dppe).

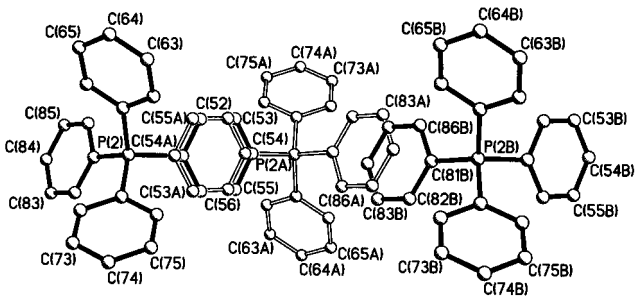

Figure 1. ORTEP view of the disordered half-occupancy PPh_4^+ ion in the $[PPh_4]_3[Mo_3I_{12}]$ structure, illustrating the infinite chain arrangement.

X-ray Crystallography for [PPh$_3$]$_3$[Mo$_3$I$_{12}$]. A dark purple, nearly black, crystal with dimensions 0.20 × 0.20 × 0.50 mm with a parallelepiped habit was placed on the Enraf-Nonius CAD4 diffractometer. The cell parameters and orientation matrix were determined by least-squares fitting of the setting angles of 25 reflections in the range $15.0 < \theta < 17.0°$; these constants were confirmed with axial photographs. The periodic monitoring of three nearly orthogonal standard reflections indicated insignificant change in intensity, showing crystal stability. An absorption correction based on seven ψ-scan reflections was applied.

Intensity statistics clearly favored the centrosymmetric space group choice. The structure was determined with the successful location of all molybdenum and iodine atoms. Subsequent difference-Fourier maps revealed the location of one full occupancy PPh_4^+ ion and another PPh_4^+ at half-occupancy. This second cation proved troublesome and rigid group refinement of the phenyl rings was found necessary not only to form planar rings but also to enable refinement of atoms found to lie nearly on top of one another. Two of the phenyl rings (C5x and C8x) and the central phosphorus atom lie in a plane that, due to crystallographic symmetry, has substantial overlap of one PPh_4^+ with its neighboring PPh_4^+ (see Figure 1). In addition, the remaining two phenyl rings (C6x and C7x) share their location with interstitial solvent molecules, which were modeled as one $^1/_2$ occupancy and two $^1/_8$ occupancy CH_2Cl_2 molecules and one $^1/_4$ occupancy Et_2O molecule. Full details of the refinement procedures are available in the Supporting Information. Hydrogen atoms were placed in calculated positions with U_H set equal to 1.2U(parent). The structure was refined to convergence with anisotropic refinement only for Mo, I, and P atoms and for the C atoms of the full occupancy PPh_4^+ cation and for the Cl atoms of the 0.5 occupancy CH_2Cl_2 molecule. A final difference-Fourier map possessed many peaks (height ≤ 1.37 e Å^{-3}) at < 1.2 Å from iodine atoms. Crystal data are listed in Table 2, and selected bond distances and angles for the $[Mo_3I_{12}]^{3-}$ ion are collected in Table 3.

Results

Generation and Characterization of the [MoX$_3$Y(THF)$_2$]$^-$ Ions. The reaction between $MoX_3(THF)_3$ and Y^- (X, Y = Cl, Br, I) was conducted in the NMR tube in $CDCl_3$ for any combination of X and Y. Within a few minutes at room temperature, a single isomer for the product $[MoX_3Y(THF)_2]^-$ was selectively formed in each case (see eq 1). The ^{1}H-NMR

$$\textit{mer}\text{-}MoX_3(THF)_3 + Y^- \rightarrow \textit{mer,trans}\text{-}[MoX_3Y(THF)_2]^- + 2THF \quad (1)$$

spectra of the products are collected in Table 1. The data show greater downfield shifts for complexes with heavier halide

Table 2. Crystal Data for $[PPh_4]_3[Mo_3I_{12}]\cdot 1.5CH_2Cl_2\cdot 0.5Et_2O$

formula	$C_{75.5}H_{68}Cl_3I_{12}Mo_3O_{0.5}P_3$
fw	2993.32
space group	P$\bar{1}$
a, Å	11.385(2)
b, Å	12.697(3)
c, Å	16.849(2)
α, deg	76.65(2)
β, deg	71.967(12)
γ, deg	84.56(2)
V, Å^3	2252.5(7)
Z	1
d_{calc}, g/cm^3	2.207
μ(Mo Kα), cm^{-1}	4.704
radiation (monochromated in incident beam)	Mo Kα ($\lambda = 0.710\ 69$ Å)
temp, K	153(2)
transmissn factors: max, min	1.000, 0.6777
R^a	0.0611
$R_w{}^b$	0.1375

^{a} $R = \sum||F_o| - |F_c||/\sum|F_o|$. ^{b} $R_w = [\sum w(|F_o| - |F_c|)^2/\sum w|F_o|^2]^{1/2}$; $w = 1/\sigma^2(|F_o|)$.

Table 3. Selected Bond Distances (Å) and Angles (deg) for $[PPh_4]_3[Mo_3I_{12}]\cdot 1.5CH_2Cl_2\cdot 0.5Et_2O$

Mo(1)−Mo(2)	3.258(2)	Mo(2)−I(2)	2.751(2)
Mo(1)−I(11)	2.7652(12)	Mo(2)−I(3)	2.757(2)
Mo(1)−I(12)	2.7798(12)	Mo(2)−I(11)	2.817(2)
Mo(1)−I(13)	2.7613(12)	Mo(2)−I(12)	2.809(2)
Mo(2)−I(1)	2.749(2)	Mo(2)−I(13)	2.825(2)
Mo(2)−Mo(1)−Mo(2)′	180.0	I(1)−Mo(2)−I(13)′	178.81(7)
I(11)−Mo(1)−I(11)′	180.0	I(2)−Mo(2)−I(3)	90.95(6)
I(11)−Mo(1)−I(12)	89.39(3)	I(2)−Mo(2)−I(11)	89.02(5)
I(11)−Mo(1)−I(12)′	90.61(3)	I(2)−Mo(2)−I(12)′	177.46(7)
I(11)−Mo(1)−I(13)	89.73(3)	I(2)−Mo(2)−I(13)′	89.98(5)
I(11)−Mo(1)−I(13)′	90.27(3)	I(3)−Mo(2)−I(11)	178.30(7)
I(12)−Mo(1)−I(12)′	180.0	I(3)−Mo(2)−I(12)′	91.03(6)
I(12)−Mo(1)−I(13)	90.30(4)	I(3)−Mo(2)−I(13)′	90.35(6)
I(12)−Mo(1)−I(13)′	89.70(4)	I(11)−Mo(2)−I(12)′	88.96(5)
I(13)−Mo(1)−I(13)′	180.0	I(11)−Mo(2)−I(13)′	87.95(5)
I(1)−Mo(2)−I(2)	90.98(6)	I(12)−Mo(2)−I(13)	88.41(5)
I(1)−Mo(2)−I(3)	90.34(6)	Mo(1)−I(11)−Mo(2)	71.40(4)
I(1)−Mo(2)−I(11)	91.36(6)	Mo(1)−I(12)−Mo(2)′	71.30(4)
I(1)−Mo(2)−I(12)′	90.60(5)	Mo(1)−I(13)−Mo(2)′	71.34(4)

ligands. The presence of only a single resonance for each type of coordinated THF proton and the analogy with the previously investigated reactions with phosphine ligands[10] indicate that the isomer formed is the *mer*,*trans*. The starting materials are known to have a *mer* geometry;[8,38,41,42] thus the THF ligand located *trans* relative to a halide ligand is probably replaced selectively, in agreement with the known trend of trans effects ($Cl^- >$ ether). For the $MoX_3(THF)_3$ compounds where X = Br or I, the situation is not expected to change because the Br^- and I^- ligands are generally considered better trans directors than Cl^-.[43] A previously reported crystallographic study confirms the trans geometry for the $[MoCl_4(THF)_2]^-$ ion.[12]

For the reaction between $MoI_3(THF)_3$ and Cl^-, the resonances assigned to the *mer*,*trans*-$[MoI_3Cl(THF)_2]^-$ ion (see Table 1) are accompanied by smaller resonances at slightly lower downfield chemical shifts (ca. δ 93 and 10.0, respectively). These resonances become more prominent when the reaction is repeated with 2 equiv of Cl^-. We assign these resonances to the product of Cl/I ligand exchange, $[MoI_2Cl_2(THF)_2]^-$, for which we propose the relative *cis*(Cl),*cis*(I),*trans*(THF) geometry on the basis of the greater trans directing ability of I^- versus Cl^-. Interestingly, a similar product is not observed in the reaction between $MoCl_3(THF)_3$ and I^-, which stops at the formation of the $[MoCl_3I(THF)_2]^-$ ion. This indicates a thermodynamic preference for Cl vs I for octahedral Mo^{3+}, which parallels the trend found for the organometallic Mo(III) system $CpMoX_2(PMe_3)_2$ (X = Cl, I).[44,45]

Continued monitoring of all these $MoX_3(THF)_3/Y^-$ reactions, however, showed that the $[MoX_3Y(THF)_2]^-$ compounds were not indefinitely stable in the $CDCl_3$ solvent used for the experiments but rather lost additional THF ligands from the coordination sphere (vide infra). Stable salts of the $[MoX_4(THF)_2]^-$ complexes (counterions were PPh_4^+, Bu_4N^+, Pr_4N^+, and PPN^+ for X = I; Bu_4N^+ and PPN^+ for X = Br) were isolated in good yields by carrying out reaction 1 in THF as solvent. In addition, the PPh_4^+ and PPN^+ salts of the $[MoCl_4(THF)_2]^-$ complex have been previously reported.[10,12]

Loss of THF from $[MoX_4(THF)_2]^-$. Dissolution of all salts of $[MoX_4(THF)_2]^-$ (X = Br, I) in CD_2Cl_2 results in the eventual loss of all coordinated THF resonances, the only new resonances appearing in the ^{1}H-NMR spectrum being those due to free THF. Integration of the latter resonances against the resonances of the corresponding counterion shows that 2 equiv of THF/mol of complex is released in each case. The complete loss of coordinated THF is also observed for the mixed halide complexes $[MoBr_nI_{4-n}(THF)_2]^-$ (n = 1, 3) made in situ by the NMR reactions described in the previous section. The decomposition of these mononuclear octahedral complexes is faster the heavier the ligands, $[MoBr_4(THF)_2]^-$ being the slowest (complete conversion in ca. 24 h at room temperature) and $[MoI_4(THF)_2]^-$ being the fastest (15 min−1 h depending on the counterion). These spectral changes are attributed to the formation of THF-free $[Mo_3Br_{3n}I_{12-3n}]^{3-}$ complexes. Salts of $[Mo_3Br_{12}]^{3-}$ and $[Mo_3I_{12}]^{3-}$ have been isolated from the direct interaction of the corresponding $MoX_3(THF)_3$ and X^- in CH_2Cl_2 (see eq 2) and the iodo trianion has been subjected to an X-ray structural determination (vide infra).

$$3MoX_3(THF)_3 + 3[Cat]^+X^- \xrightarrow{CH_2Cl_2} [Cat]_3[Mo_3X_{12}] + 9THF \quad (2)$$

$$X = Br,\ Cat = Bu_4N,\ PPN$$

$$X = I,\ Cat = PPh_4,\ Bu_4N,\ Pr_4N,\ PPN$$

For the $MoI_3(THF)_3/I^-$ reaction, monitoring for a longer period of time (3 days) showed the slow appearance of two resonances in a 1:1 ratio at δ 3.3 and 2.0 (intensity ca. 10% of the intensity of the free THF resonances at δ 3.75 and 1.85). These resonances correspond to 1,4-diiodobutane, which probably arises from a secondary reaction that involves oxygen abstraction from THF by the unsaturated Mo(III) center. Oxygen abstraction from THF by low-valent molybdenum iodide systems has been reported before.[46]

Contrary to the tetrabromo, tetraiodo, and mixed bromoiodo complexes, the tetrachloro $[MoCl_4(THF)_2]^-$ complex does not lose all the THF upon prolonged treatment in dichloromethane. Rather, only 1.5 equiv of THF per Mo atoms are released and new slightly paramagnetically shifted resonances for coordinated THF, corresponding to the remaining 0.5 equiv of THF, grow in the ^{1}H-NMR spectrum at δ 6.5 and 2.2 (1:1 ratio). Both the stoichiometry and the similarity with the loss of THF from

(41) Hofacker, P.; Friebel, C.; Dehnicke, K.; Bäuml, P.; Hiller, W.; Strähle, J. *Z. Naturforsch.* **1989**, *44b*, 1161.
(42) Calderazzo, F.; Maichle-Mössmer, C.; Pampaloni, G.; Strähle, J. *J. Chem. Soc., Dalton Trans.* **1993**, 655.
(43) Huheey, J. E. *Inorganic Chemistry. Principles of Structure and Reactivity;* 4th ed.; Harper & Row: New York, 1993.
(44) Linck, R. G.; Owens, B. E.; Poli, R.; Rheingold, A. L. *Gazz. Chim. Ital.* **1991**, *121*, 163.
(45) Poli, R.; Owens, B. E.; Linck, R. G. *Inorg. Chem.* **1992**, *31*, 662.
(46) Cotton, F. A.; Poli, R. *Polyhedron* **1987**, *6*, 2181.

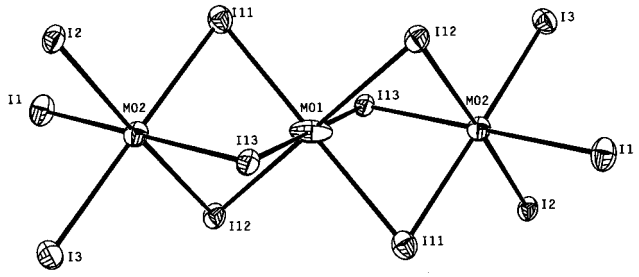

Figure 2. ORTEP view of the $[Mo_3I_{12}]^{3-}$ anion in compound $[PPh_4]_3[Mo_3I_{12}]$ with the labeling scheme employed. Ellipsoids are drawn at the 40% probability level.

$MoCl_3(THF)_3$ to afford $Mo_2Cl_6(THF)_3$, indicate that $[MoCl_4(THF)_2]^-$ converts to the $[Mo_2Cl_8(THF)]^{2-}$ ion (eq 3). The

$$2[MoCl_4(THF)_2]^- \xrightarrow{CH_2Cl_2} [Mo_2Cl_8(THF)]^- + 3THF \quad (3)$$

position of the ^{1}H-NMR resonances for coordinated THF in $[Mo_2Cl_8(THF)]^{2-}$ is very similar to those in the face-sharing bioctahedral $Mo_2Cl_6(THF)_3$,[38] indicating that the two molecules have very similar magnetic properties. Therefore, the structure of this dianion is most probably also a face-sharing bioctahedron, e.g. $[Cl_3Mo(\mu\text{-}Cl)_3MoCl_2(THF)]^{2-}$. The structure of an analogous phosphine derivative, $[Cl_3Mo(\mu\text{-}Cl)_3MoCl_2(PEt_3)]^{2-}$, has recently been reported.[47]

During the monitoring of the THF loss from $[MoCl_4(THF)_2]^-$, a weak paramagnetically shifted resonance at δ 17 is also observed. This is assigned to the a THF protons of an edge-sharing $[Mo_2Cl_8(THF)_2]^{2-}$ intermediate with equivalent THF ligands, by analogy with the $Mo_2Cl_6(THF)_4$ intermediate observed during the transformation of $MoCl_3(THF)_3$ to $Mo_2Cl_6(THF)_3$.[38] The corresponding β-H resonance could not be clearly identified due to the low intensity and the probable overlap with stronger resonances in the diamagnetic region. For edge-sharing $Mo_2Cl_6(THF)_4$, two sets of 1:1 resonances were observed at 25.0 and 19.7 ppm for α-H and at 3.7 and 3.4 ppm for β-H.[38]

X-ray Structure of $[PPh_4]_3[Mo_3I_{12}]$. Compound $[PPh_4]_3[Mo_3I_{12}]$ crystallizes in the triclinic P$\bar{1}$ group with the trianion residing on a crystallographic inversion center. One PPh_4^+ is located on a general position, while another exhibits an unusual kind of symmetry-related disorder: the ion is located at half-occupancy on a general position about halfway between two crystallographic inversion centers to generate an infinite chain of ions (see Figure 1). Two phenyl rings for each ions are almost overlapping with the phenyl rings of the two neighbors in the chain. No further comment is deserved by the cations. A view of the trianion is shown in Figure 2. The structure can be conveniently described as a linear face-sharing trioctahedron; i.e. each metal is surrounded by six iodide ligands in an octahedral configuration and the three octahedra share triangular faces to form a linear arrangement of the metal atoms. This is only the second such linear trioctahedral structure for a dodecahalotrimetalate ion, the first one being that of $[Ru_3Cl_{12}]^{4-}$ and reported 16 years ago by Bino and Cotton.[48] Later, Cotton and co-workers have also reported several linear trioctahedral phosphine derivatives of Ru_3^{7+}, Ru_3^{8+}, and Ru_3^{9+}.[49−51]

A Mo2−Mo1−Mo2′ angle of 180° is imposed by the crystallographic inversion center. As expected, the terminal Mo−I bonds (average 2.752(4) Å) are shorter than the bridging Mo−I bonds. Unexpectedly, though, there is a large disparity between the Mo−(μ-I) bonds to the central Mo atom (average 2.769(10) Å) and those to the two lateral Mo atoms (average 2.817(7) Å). For comparison, the average terminal and bridging Mo−I distances (trans to I) are 2.758 and 2.813 Å for compound $[Mo_2I_6(\mu\text{-}I)_2(\mu\text{-}H)]^{3-}$ and 2.763 and 2.764 Å for compound $[Mo_2I_4(PMe_3)_2(\mu\text{-}I)_3]^-$.[28,52] Another interesting and, we believe, significant feature of this structure is the shape of the thermal ellipsoid for the central Mo atom (see Figure 2). This shape cannot result from problems inherent to the refinement of intensity data, such as anomalous absorption and extintion, because these problems would equally affect the shape of the ellipsoids of the other heavy atoms and this is not the case as clearly shown in Figure 2. Rather, the ellipsoid of Mo1 is indicative of a dynamic libration of the Mo1 atom between two equivalent positions on either side of the inversion center, toward the Mo1 and Mo1′ positions.

The most interesting parameters are those related to the compression or elongation of the trioctahedron along the molecular axis defined by the Mo−Mo vectors, which gives an indication about attractive or repulsive interactions between adjacent metal atoms. As detailed in the classical contribution of Cotton and Ucko,[53] an ideal edge-sharing bioctahedron is characterized by a M−(μ-X)−M angle of 70.53°, and when a metal−metal bonding interaction is not present, a much larger angle results as a consequence of the repulsive interaction (angles greater than 80° are typically found for molecules having no metal−metal bond).[53] Thus, the average Mo−I−Mo angle of 71.34(7)° in the $[Mo_3I_{12}]^{3-}$ ion indicates that metal−metal interactions are present. This angles are smaller than those reported for the trioctahedral metal−metal bonded ruthenium complexes $[Ru_3Cl_{12}]^{4-}$, $Ru_3Cl_8(PR_3)_4$, and $[Ru_3Cl_8(PR_3)_4]^+$ (in the 72−75° range).[49−51] The above parameters are more indicative of metal−metal attractive interactions than the actual metal−metal distance (3.258(2) Å), since this is strongly affected by the large size of the bridging iodide ligands. The octahedral coordination geometry around the central Mo atom is almost ideal: the (μ-I)−Mo1−(μ-I) angles average 90.4(2)° when relating I atoms on the same shared face and 89.6(2)° when relating *cis* I atoms on the two opposite shared faces. On the other hand, the octahedra around the two lateral Mo atoms show a greater distortion: while the I−Mo−I angles are close to the ideal 90° value (average 90.4(2)°), the (μ-I)−Mo−(μ-I) angles are significantly more closed (average 88.4(5)°). The most significant comparison of the above structural parameters is with the triply iodo-bridged face-sharing bioctahedral $[Mo_2I_7(PMe_3)_2]^-$ ion[28] and with the $[Mo_2I_9]^{3-}$ ion.[54] The $[Mo_2I_7(PMe_3)_2]^-$ ion shows smaller Mo−I−Mo angles (65.8 and 65.9° for the $PHMe_3$ and $AsPh_4$ salts, respectively) and a shorter Mo−Mo distance (3.021(4) and 3.022(1) Å for the same salts), and similar parameters are found for $Cs_3Mo_2I_9$ (Mo−I−Mo: 68.1(5)°; Mo−Mo, 3.07(2) Å). In conclusion, the structural data indicate that there is a direct metal−metal bonding interaction present in $[Mo_3I_{12}]^{3-}$, although this is weaker than the interaction present in $[Mo_2I_7(PMe_3)_2]^-$ and in $[Mo_2I_9]^{3-}$. A simple theoretical analysis, which is presented later in the Discussion, fully rationalizes these observations.

Other Characterization of the $[Mo_3X_{12}]^{3-}$ Complexes. Vibrational Spectra. The molecular D_{3d} symmetry of the $[Mo_3X_{12}]^{3-}$ ions leads to the prediction of two IR-active bands

(47) Vidyasagar, K. *Inorg. Chim. Acta* **1995**, *229*, 473.
(48) Bino, A.; Cotton, F. A. *J. Am. Chem. Soc.* **1980**, *102*, 608.
(49) Cotton, F. A.; Matusz, M.; Torralba, R. C. *Inorg. Chem.* **1989**, *28*, 1516.
(50) Cotton, F. A.; Torralba, R. C. *Inorg. Chem.* **1991**, *30*, 3293.
(51) Cotton, F. A.; Torralba, R. C. *Inorg. Chem.* **1991**, *30*, 4386.
(52) Bino, A.; Luski, S. *Inorg. Chim. Acta* **1984**, *86*, L35.
(53) Cotton, F. A.; Ucko, D. A. *Inorg. Chim. Acta* **1972**, *6*, 161.
(54) Stranger, R.; Grey, I. E.; Madsen, I. C.; Smith, P. W. *J. Solid State Chem.* **1987**, *69*, 162.

($A_{2u} + E_u$) for the terminal Mo−X stretching vibrations and four IR-active bands ($2A_{2u} + 2E_u$) for the Mo−(μ-X) vibrations. Correspondingly, terminal and bridging Mo−X bonds should give rise to two ($A_{1g} + E_g$) and four ($2A_{1g} + 2E_g$) Raman active bands. Four cation independent bands are observed in the IR, and two bands are observed in the Raman spectrum for the iodide salts, between 250 and 100 cm^{-1}. The complete mismatch between IR and Raman bands is consistent with the inversion symmetry of the ion. The bromides salts were only investigated by IR pectroscoopy, affording low-energy bands between 260 and 200 cm^{-1}. As stated in the Introduction, a salt of the corresponding chloro complex, $[Mo_3Cl_{12}]^{3-}$ was reported several years ago by Wentworth.[37] This compound also shows only four stretching vibrations (rather than the expected six) in the Mo−Cl stretching region, probably because of accidental overlap. Following the detailed analysis offered for that trinuclear complex (for which a comparison with dinuclear $[Mo_2Cl_9]^{3-}$ ion was possible), the two IR bands at higher frequency are assigned to the vibration of terminal bonds and those at lower frequency to bridging bonds.

Magnetic Properties. An interesting feature of the $[Mo_3X_{12}]^{3-}$ salts is their magnetic moment, which is 3.17 μ_B (1.83 μ_B/Mo atom) for $[PPh_4]_3[Mo_3I_{12}]$, 3.36 μ_B (1.94 μ_B/Mo atom) for $[NPr_4]_3[Mo_3I_{12}]$, and 2.60 μ_B (1.50 μ_B/Mo atom) for $[PPh_4]_3[Mo_3Br_{12}]$ at room temperature. These values are much smaller than expected on the basis of three unpaired electron per metal atom and therefore indicate considerable electron pairing between the t_{2g}^3 configurations of the three ideal octahedra. For comparison, the previously reported tetra-*n*-butylammonium salt of $[Mo_3Cl_{12}]^{3-}$ shows a moment of 2.02 μ_B at 302 K and 1.34 μ_B at 103 K (or 1.17 and 0.77 μ_B/Mo atom, respectively).[37]

The temperature-dependent magnetic data for $[PPh_4]_3[Mo_3I_{12}]$ show a gradual decrease in the effective magnetic moment as the temperature is lowered from room temperature. From the analysis of the electronic structure (see Discussion) and crystal structure, a magnetic model consisting of a linear arrangement of Mo^{3+} ions with available spin quantum numbers of $S = 1$ for the outer two ions and $S = {}^3/_2$ for the central ion was used. The spin Hamiltonian for a trinuclear system is given in eq 4, where $S_1 = S_3 = 1$ and $S_2 = {}^3/_2$. The magnetic

$$H = -2J_a[(S_1S_2) + (S_2S_3)] - 2J_b(S_1S_3) \quad (4)$$

$$\chi = -\frac{N}{H}\frac{\sum\left(\frac{dE_i}{dH}\right)e^{-E_i/kT}}{\sum e^{-E_i/kT}} \quad (5)$$

susceptibility may be calculated from the calculated energies obtained from the spin Hamiltonian shown in eq 4, using the relationship shown in eq 5.

In order to successfully analyze the data, we must correct the magnetic data for secondary magnetic exchange interactions using the molecular exchange field. The equation that describes the effect of a molecular exchange field on the magnetic susceptibility is

$$\chi = \frac{\chi'}{1 - \frac{2zJ'}{N_g{}^2\mu_B{}^2\chi'}} + \mathrm{TIP} \quad (6)$$

where χ' is the magnetic susceptibility of the material in the absence of the exchange field and χ is the molecular exchange field influenced magnetic susceptibility that is actually measured. The exchange field coupling parameter is zJ', where z is the number of exchange coupled neighbors. The addition of the molecular field exchange correction resulted in a substantial improvement of the fit to the data. The temperature dependence of the magnetic susceptibility was determined using the numerical calculated susceptibility from eq 5 corrected with eq 6. A calculation of the magnetic susceptibility for this model was then used to analyze the behavior of the two compounds. A least-squares fit of the effective magnetic moment to eq 4 gave the parameters $g = 2.419$, $J_a/k = -749$ K, $J_b/k = 7.3$ K, $zJ'/k = -0.97$ K, and TIP = 0.00133 emu/mol for $[PPh_4]_3[Mo_3I_{12}]$ and $g = 1.763$, $J_a/k = -480$ K, $J_b = -3.9$ K, $zJ'/k = -233$ K, TIP = 0.00158 emu/mol for $[PPh_4]_3[Mo_3Br_{12}]$. The magnetic analysis for the bromide analysis does not give as good a fit to the data as the iodide complex. The data and fit for the iodide complex are shown in Figure 3.

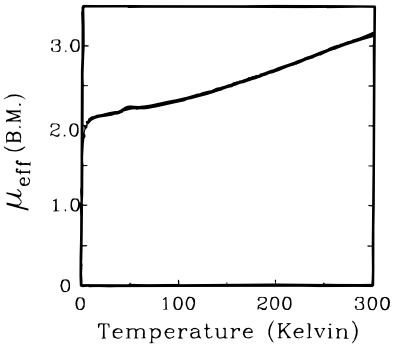

Figure 3. Effective magnetic moment of $[PPh_4]_3[Mo_3I_{12}]$ plotted as a function of temperature over the 1.7−300 K temperature region. The line drawn through the data is the fit to the Curie−Weiss model as described in the text.

Optical Spectra. The previously reported $[Mo_3Cl_{12}]^{3-}$ shows optical features that are characteristic of octahedral $Mo^{III}Cl_6$ coordination;[37] thus we were naturally interested in obtaining comparable information for the trinuclear Br and I complexes. Unfortunately, further chemical transformations complicate the measurement of the optical spectra for the $[Mo_3X_{12}]^{3-}$ (X = Br, I) ions. When CH_2Cl_2 solutions of $[Mo_3X_{12}]^{3-}$ (X = Br, I) salts are freshly prepared and immediately measured, no distinctive absorptions are observed in the visible and near-UV region. The colors of the complexes are due to intense UV absorption that tail into the visible region. Continued measurements after exposing these solutions to air revealed the growth of bands in the visible region. These are centered at 665 and 526 nm for X = I and at 426 and 384 nm for X = Br. The intensity of these new bands grows at a considerably faster rate for the bromide system than for the iodide system. The bands are assigned, by comparison with a genuine sample for the iodo system,[55] to the oxomolybdenum(V) complexes $[MoOX_4]^-$ formed by air oxidation of $[Mo_3X_{12}]^{3-}$ salts.

Loss of X^- and Formation of Triangular Trimers. In addition to the sensitivity toward oxygen, the solution chemistry of complexes $[Mo_3X_{12}]^{3-}$ is also complicated by loss of halide ions. In early attempts to grow single crystals of the $[PPh_4]_3[Mo_3I_{12}]$ compound, after a long residence time in the crystallization solvent (CH_2Cl_2/pentane), single crystals were obtained for the *n*-Bu_4N^+ salt, one of which was investigated by X-ray analysis. Severe disorder both in the cations and in the anion prevented a satisfactory refinement of the structure, which is therefore described only qualitatively. There is no doubt, however, that the compound corresponds to a salt of the $[Mo_3I_{10}X]^{2-}$ ion (see drawing **I**), where X stands for a

(55) Gordon, J. C.; Mattamana, S. P.; Poli, R.; Fanwick, P. E. *Polyhedron* **1995**, *14*, 1339.

compositional disorder of Cl and I, the Cl atom probably originating from the solvent.

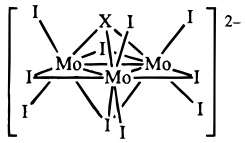

I

The structure, which is not unprecedented,[56] shows an octahedral coordination geometry around each Mo center, just as in the $[Mo_3I_{12}]^{3-}$ precursor, but this time the three octahedra are conpenetrating: each pair of adjacent octahedra share a triangular face which is identified by the bridging and the two capping ligands. This conpenetration process causes a much greater distortion of the octahedral geometry with respect to the linear trioctahedral structure (especially the cap−Mo−cap angles which are much greater than 90°), and this may well be the reason for the tendency to incorporate the smaller Cl atom in the structure. We therefore suppose that an equilibrium of halide loss such as that shown in eq 7 might take place in

$$[Mo_3X_{12}]^{3-} \rightleftarrows [Mo_3X_{11}]^{2-} + X^- \qquad (7)$$

solution. The addition to these solutions of the halide scavenger Tl^+ immediately affords insoluble precipitates (off-white for Br, yellow for I, presumably TlX), in support of the presence of free X^- in solution. We have so far been unable to isolate analytically pure samples of the trimolybdenum product or to grow less disordered single crystals relative to that of the *n*-Bu_4N^+ species discussed above.

The initial failure to grow single crystals of $[PPh_4]_3[Mo_3I_{12}]$ could possibly be ascribed to the presence in solution of the various species generated by equilibrium 7. The successful crystallization of this compound was eventually possible from solutions containing an excess of PPh_4I, which supposedly keeps the equilibrium on the left-hand side of eq 7.

Reaction of $[Mo_3X_{12}]^{3-}$ with Phosphines. The reaction between the trinuclear ions and the ligands PMe_3 and dppe has been investigated by ^{1}H-NMR spectroscopy. The anticipated product $[MoX_4L_2]^-$ (L_2 = dppe or L = PMe_3) formed, but the reaction was not selective as expected, other phosphine derivatives being also formed as shown in eqs 8 and 9. This result

$$[Mo_3X_{12}]^{3-} + PMe_3\ (2\ \text{equiv/Mo}) \rightarrow [MoX_4(PMe_3)_2]^- + MoX_3(PMe_3)_3 + [Mo_2X_7(PMe_3)_2]^- \qquad (8)$$

$$[Mo_3X_{12}]^{3-} + dppe\ (1\ \text{equiv/Mo}) \rightarrow [MoX_4(dppe)]^- + Mo_2X_6(dppe)_2 \qquad (9)$$

might simply reflect a kinetic control of the reaction. In the case of the reaction with PMe_3, we observed the formation of the same products in approximately the same proportions from either the isolated $[Mo_3I_{12}]^{3-}$ salts or from solutions of the trinuclear trianion obtained in situ by THF loss from $[MoI_4(THF)_2]^{2-}$. However, the interaction between the latter compound and PMe_3 under conditions that minimize the THF loss process to the trinuclear species results in the increase of the relative amount of the $[MoI_4(PMe_3)_2]^-$ ion and the decrease of the relative amount of the other products.

The ^{1}H-NMR spectra of $MoX_3(PMe_3)_3$ have been previously reported.[22] The $[MoI_4(PMe_3)_2]^-$ ion has been independently synthesized and isolated by exchange of THF with PMe_3 from $[PPh_4][MoI_4(THF)_2]$. Its contact-shifted PMe_3 ^{1}H-NMR resonance is observed at δ −41.2, which compares with the previously reported resonance of $[MoCl_4(PMe_3)_2]^-$ at δ −39.[10] The corresponding bromide compound has not been isolated. Its resonance is observed at δ −40.8, namely between the values observed for the related Cl and I ions. Finally, the $[Mo_2X_7(PMe_3)_2]^-$ (X = Cl, I) ions have been previously characterized by ^{1}H-NMR,[28,29] and the $[Mo_2Br_7(PMe_3)_2]^{2-}$ ion is identified by its resonances at δ −1.2 and −1.7 (for the *anti* and *gauche* isomers, respectively), ca. halfway between those of the corresponding iodo complexes at δ −2.18 and −2.84[28] and those of the chloro complexes at δ −0.61 and −0.71.[29] The only other resonances observed during these ^{1}H-NMR experiments are sharp ones with halide-independent chemical shifts of δ 2.2 and 1.8. These are due to the product of the reaction between PMe_3 and the solvent CH_2Cl_2, e.g. $[Me_3PCH_2Cl]^+$, as confirmed by a control experiment.

For the reaction with dppe, eq 9, the major observed product is $[MoX_4(dppe)]^-$. Compound $[PPh_4][MoI_4(dppe)]$ has been previously synthesized and characterized.[57] The identity of the $[MoBr_4(dppe)]^-$ ion is based on the similarity of the resonances attributed to this ion with those observed for the $[PPh_4][MoI_4(dppe)]$. The $[MoBr_4(dppe)]^-$ ion has also been previously reported, but it has only been characterized by X-ray crystallography as the $[Bu_4N]^+$ salt.[58] We have independently synthesized the $[MoBr_4(dppe)]^-$ ion in high yields by reacting $MoBr_3$(dppe)THF with PPNBr in CH_2Cl_2. The identity of the dinuclear species $Mo_2X_6(dppe)_2$ (X = Br, I) is based on the similarity of the ^{31}P-NMR resonances attributed to these ions at δ −35.73 (X = I) and δ −39.92 (X = Br) with that reported for $Mo_2Cl_6(dppe)_2$ at δ 42.96.[59]

Discussion

The loss of THF in noncoordinating solvents from the easily accessible $[MoX_4(THF)_2]^-$ complexes provides a convenient entry into face-sharing trioctahedral $[Mo_3X_{12}]^{3-}$. The chloride complex had previously been obtained by a different method and proposed to adopt a linear face-sharing trioctahedral structure. With the new synthetic method described here, we have gained entry into the corresponding heavier halide derivatives and we have verified by X-ray crystallography that the structure adopted by $[Mo_3I_{12}]^{3-}$ indeed corresponds to the early proposal made by Wentworth for the chloride analogue.

It is appropriate to give a qualitative description of the metal−metal bonding in this class of compounds since this was not done by Wentworth, although the scheme is analogous (but with a different number of available metal electrons) to that provided by Bino and Cotton for the diamagnetic ruthenium analogue $[Ru_3Cl_{12}]^{4-}$.[48] As shown by the metal−metal distance and by angular parameters (see Results) in comparison with those in the face-sharing bioctahedral complexes $[Mo_2I_7(PMe_3)_2]^-$ and $[Mo_2I_9]^{3-}$, a metal−metal bonding interaction is present in the trinuclear complex but this is weaker than for the dinuclear complexes. Another important consideration relates to the molecular and electronic structure and magneto−structural correlations in face-sharing bioctahedral $[Mo_2X_9]^{3-}$ complexes, including that with X = I, which have recently been investigated in great detail.[32,33] It has been found that the magnetic properties can appropriately be described by considering two electrons as fully paired in a strong metal−metal σ bond, and the other two

(56) Professor R. McCarley has informed us of the crystallographic characterization of a salt of $[Mo_3Cl_{11}]^{2-}$ in his laboratory.

(57) Mattamana, S. P.; Poli, R. *Inorg. Chim. Acta* **1995**, *229*, 55.
(58) Salagre, P.; Sueiras, J.-E.; Solans, X.; Germain, G. *J. Chem. Soc., Dalton Trans.* **1985**, 2263.
(59) Poli, R.; Owens, B. E. *Gazz. Chim. Ital.* **1991**, *121*, 413.

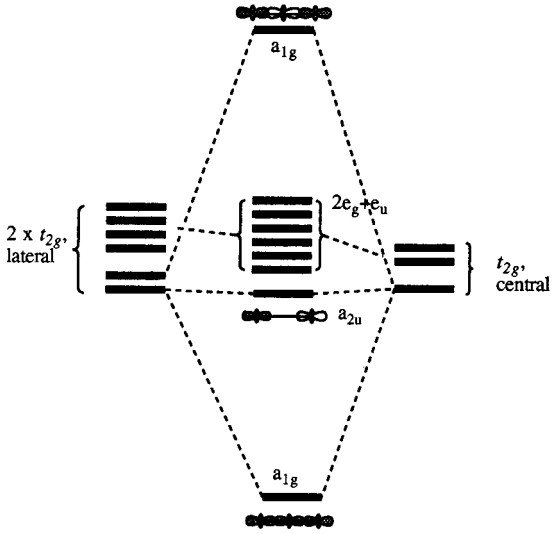

Figure 4. Qualitative MO diagram for the metal orbital region of $[Mo_3X_{12}]^{3-}$.

electrons per metal (located in orbitals of π/d symmetry) being active in an exchange-coupling process that can be modeled by a modified Heisenberg−Dirac−Van Vleck spin Hamiltonian.[33]

For the trinuclear $[Mo_3X_{12}]^{3-}$ systems, each metal provides the same number of electrons and orbitals as in the dinuclear $[Mo_2X_9]^{3-}$ complexes. It is therefore reasonable to propose that, as for the dinuclear bioctahedral complexes, the σ interactions will be contributing the most to the attractive forces between the metal atoms while the other electrons will contribute little to metal−metal bonding and will be mostly responsible for the observed magnetic properties. The bonding scheme shown in Figure 4 follows directly from these considerations. The same qualitative scheme was presented for the linear trioctahedral $[Ru_3Cl_{12}]^{4-}$ complex[48] and later confirmed by SCF−Xα−SW and Fenske−Hall MO calculations.[60] There is, therefore, a low-energy σ bonding orbital and the corresponding high-energy σ antibonding orbital (both of a_{1g} type), plus one σ (a_{2u}) and six π/d ($2e_g + e_u$) essentially nonbonding orbitals at intermediate energy. The only difference between the electronic structures of the Ru_3^{8+} and the Mo_3^{9+} ions is that all seven intermediate-energy orbitals are full in the former, whereas they contain only seven electrons in the latter. However, since these orbitals provide little or no contribution to metal−metal bonding, the metal−metal interaction in the Mo complex can be described at least to a first approximation as being identical to that of the Ru species, i.e. giving rise to equivalent Mo−Mo bonds of order 0.5, in agreement with the results of the structural determination of the $[Mo_3I_{12}]^{3-}$ ion.

The observed magnetic properties of the $[Mo_3X_{12}]^{3-}$ salts are in qualitative agreement with this picture. A reduced moment is observed with respect to the nine d electrons of the three octahedral Mo(III) centers and even with respect to the seven electrons remaining after formation of the delocalized Mo−Mo bonds. The decrease of the magnetic moment as temperature decreases is fully consistent with exchange-coupling interactions of the remaining seven electrons, whereas the greater moment observed for the heavier halogen-substituted ions is consistent with the larger metal−metal separation expected for such ions, resulting in a smaller energy spread of the seven nonbonding metal orbitals.

In principle, the low-temperature limiting value of the magnetic susceptibility should correspond to a single unpaired electron ($\mu_{eff} = 1.73\ \mu_B$) for the trinuclear unit. The low-temperature-limiting value for the iodo complex is reasonably close to this expectation (see Figure 3). However, the same value for the bromo system is much lower, e.g. 0.65 μ_B. A possible explanation of this phenomenon, as it has already been advanced by Wentworth for the chloro system, is intermolecular antiferromagnetic coupling. This was indicated by the measurement of a higher magnetic moment in solution with respect to the solid state.[37] In this respect, it is reasonable to expect a greater interaction for the complexes with the smaller halide ions, allowing a closer contact between the metal centers in different trinuclear units. In addition, the smaller halide ion should also favor antiferromagnetic exchange between adjacent metal center within the same trinuclear cluster. The observed trend for the room temperature magnetic moments for the different $[Mo_3X_{12}]^{3-}$ salts, i.e. 3.17 μ_B for X = I (PPh_4^+ salt), 2.60 μ_B for X = Br (PPh_4^+ salt), and 2.02 μ_B for X = Cl (for the previously reported $NBu^n{}_4^+$ salt)[37] can then be attributed to the increase of either or both intermolecular and intramolecular antiferromagnetic exchange interactions as the size of the halide ligands becomes smaller. The same trend was also observed by magnetic susceptibility[33] and by NMR methods[27] on halide-bridged face-sharing bioctahedral complexes.

The reaction of the $[Mo_3X_{12}]^{3-}$ ions with phosphine ligands has afforded only products of lower nuclearity, probably because the rupture of the bridging Mo−X bonds and the weak Mo−Mo bond is more favorable than the exchange of the terminal halide ions. Trinuclear Mo derivatives with neutral ligands in terminal positions akin the trialkylphosphine Ru derivatives described by Cotton et al.[49−51] should be stable systems, and the THF-loss synthetic strategy described in this paper might provide a possible synthetic strategy to a wide variety of them. Linear trioctahedral complexes could also be obtained by this strategy for other metals.

Acknowledgment. We are grateful to the National Science Foundation (PYI Award 1990−95) and to the Alfred P. Sloan Foundation (Research Fellowhip 1992−94) for support of this work.

Supporting Information Available: Text giving a detailed description of data collection and structure solution and refinement and full tables of crystal parameters, fractional atomic coordinates, bond distances and angles, anisotropic thermal parameters, and H atom coordinates for $[PPh_4]_3[Mo_3I_{12}]$ (14 pages). Ordering information is given on any current masthead page.

(60) Bursten, B. E.; Cotton, F. A.; Fang, A. *Inorg. Chem.* **1983**, *22*, 2127.

IC9607301